**Figure S1. Absolute quantification of basal epithelial cells and luminal epithelial cells after treatment with MLN0128. (A)** Quantification of basal epithelial cells in vehicle or MLN0128 treated PTEN[L/L] mice (n = 6 mice per treatment arm, *P<0.0001, t-test). **(B)** Quantification of luminal epithelial cells in vehicle or MLN0128 treated PTEN[L/L] mice (n = 6 mice per treatment arm, n.s. = not statistically significant). Data are mean +/- S.E.M.
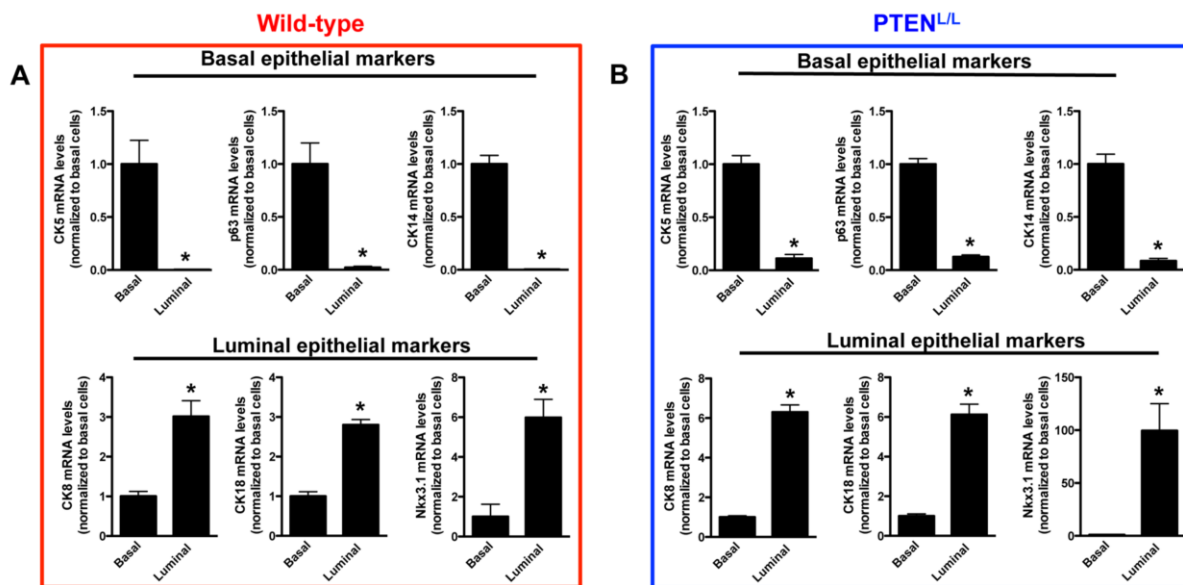

Figure S2. qPCR phenotyping of distinct sorted epithelial cell populations in wild-type and PTEN[L/L] mice. (A) qPCR-based phenotyping of sorted wild-type (WT) basal and luminal epithelial cells (representative replicate of 3 experiments, *P<0.05, t-test). **(B)** qPCR-based phenotyping of sorted PTEN[L/L] basal and luminal epithelial cells (representative replicate of 2 experiments, *P<0.05, t-test). All samples were first normalized to actin then to expression in basal cells. n.s. = not statistically significant. Data are mean +/- S.E.M.
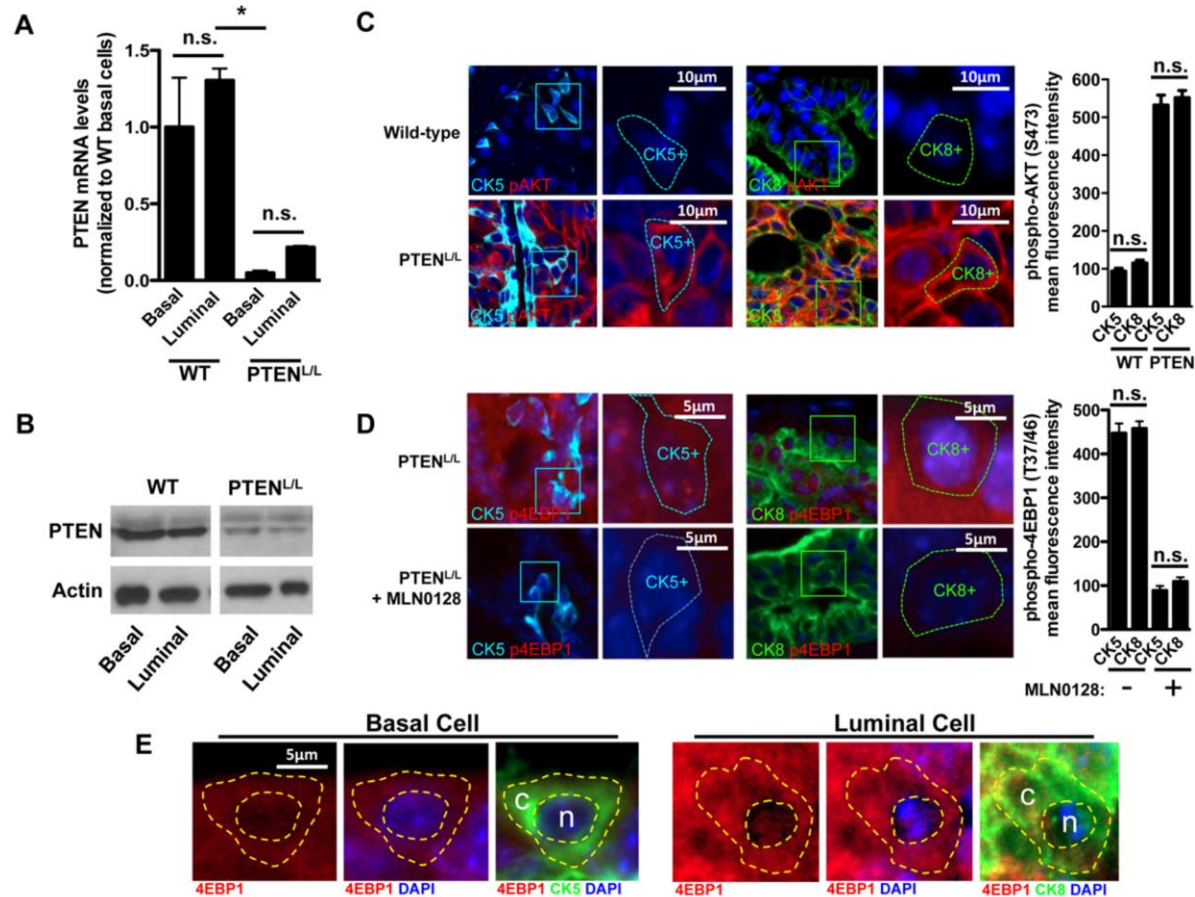
Figure S3. Efficiency of *PTEN* deletion and the phosphorylation and localization of 4EBP1 in basal and luminal epithelial cells in vivo. (A) *PTEN* mRNA expression in sorted luminal and basal epithelial cells from wild-type (WT) and PTEN[L/L] mice (n = 2 mice/genotype, *P<0.05, ANOVA). **(B)** Representative Western blot for PTEN run on the same gel in sorted luminal and basal epithelial cells from WT and PTEN[L/L] mice. **(C)** Quantitative immunofluorescence of phosphorylated AKT (Ser[473]) abundance in basal (CK5+) or luminal (CK8+) epithelial cells of WT and PTEN[L/L] mice. Left panels: representative images of basal (CK5+) and luminal (CK8+) epithelial cells co-stained with a phospho-AKT specific antibody and DAPI. Right panel: quantification of phosphorylated AKT mean fluorescence intensity in basal (CK5+) or luminal (CK8+) epithelial cells (n = 3 mice/genotype, ANOVA). Scale bar, 10 μm. **(D)** Quantitative immunofluorescence of phospho-4EBP1 (Thr[37/46]) in basal (CK5+) or luminal (CK8+) epithelial cells of PTEN[L/L] vehicle- or MLN0128-treated (1 mg/kg daily) mice. (n = 3 mice/treatment group, ANOVA). Scale bar, 5 μm. **(E)** Representative immunofluorescence image of 4EBP1 protein localization in PTEN[L/L] basal and luminal epithelial cells (c = cytoplasm, n = nucleus). Scale bar, 5 μm. n.s. = not statistically significant. Data are mean +/- S.E.M.
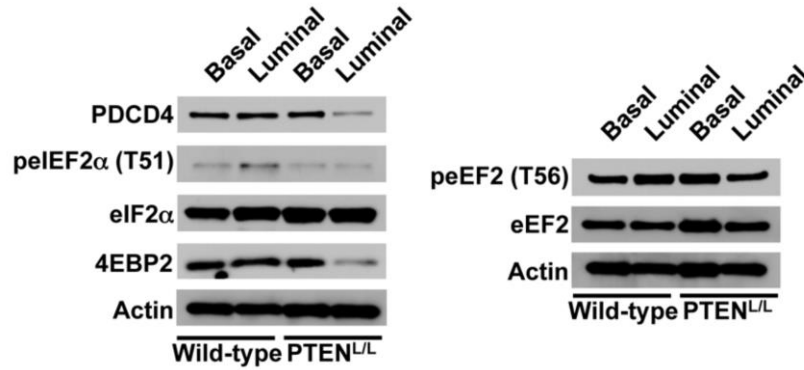
Figure S4. Western blot analysis of translation initiation factors and regulators in wild-type and PTEN^{L/L} basal and luminal epithelial cells. Representative blots for phosphorylated (Thr^{56}) and total eEF2, PDCD4, phosphorylated (Thr^{51}) and total eIF2α, and 4EBP2 in sorted prostate basal and luminal epithelial cells from age-matched wild-type and PTEN^{L/L} mice.
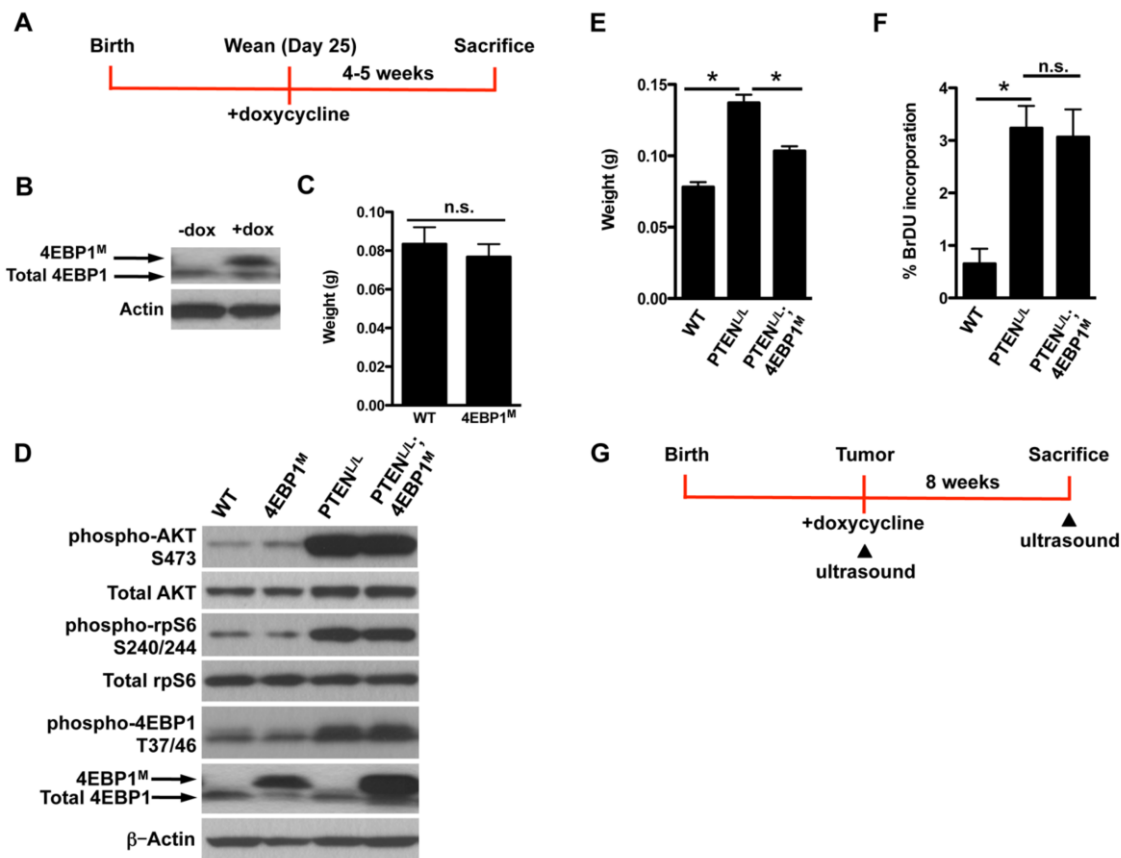

Figure S5. 4EBP1^M does not affect normal prostate homeostasis but impedes prostate cancer initiation and progression. (A) Timeline to test the impact of inhibition of eIF4E activity on normal prostate gland tissue maintenance and prostate epithelial tumor initiation, in which

the 4EBP1^M mutant transgene was expressed immediately upon weaning for 4-5 weeks. Mice were at 8-10 weeks of age at necropsy. **(B)** Representative Western blot analysis for total 4EBP1 in prostates from wild-type (WT) and 4EBP1^M mice. **(C)** Prostate weights after a 4 week treatment with doxycycline (n = 3 mice/genotype, t-test). **(D)** Representative Western blot analysis in whole prostate lysates from WT, 4EBP1^M, PTEN$^{L/L}$, and PTEN$^{L/L}$;4EBP1^M mice. **(E)** Weights of WT, PTEN$^{L/L}$, and PTEN$^{L/L}$;4EBP1^M prostates after 4-5 weeks of doxycycline treatment (n = 9-10 mice/genotype, *P < 0.05, ANOVA). **(F)** Percent BrdU incorporation by fluorescence-activated cell sorting (FACS) of whole prostates from WT, PTEN$^{L/L}$, and PTEN$^{L/L}$;4EBP1^M mice after 4-5 weeks of treatment with doxycycline after weaning (n = 5-6 mice/genotype, *P<0.05, ANOVA). **(G)** Timeline of 4EBP1^M induction in mice with established tumors to test the impact of inhibition of eIF4E activity on prostate cancer progression. Ultrasounds to assess tumor size were taken just before exposure to doxycycline and again at euthanasia. Doxycycline was administered in the drinking water at 2g/L. n.s. = not statistically significant. Data are mean +/- S.E.M.
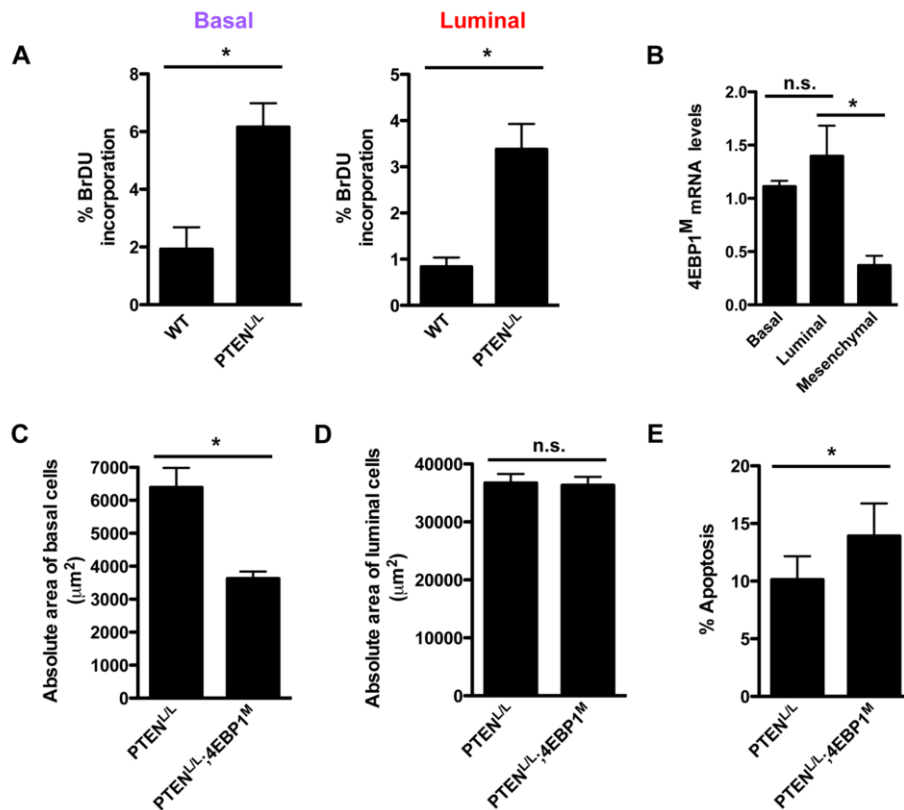
Figure S6. Effect of PTEN loss and 4EBP1^M expression on absolute number of basal and luminal epithelial cells. **(A)** Percent BrdU incorporation by fluorescence-activated cell sorting (FACS) of the basal and luminal epithelial cell types from wild-type and PTEN$^{L/L}$ mice (n = 5-6 mice/genotype, *P<0.05, t-test). **(B)** qPCR of 4EBP1^M mRNA expression in basal and luminal prostate epithelial cells in PTEN$^{L/L}$;4EBP1^M mice. Mesenchymal cells = negative control (n = 3

mice, *P <0.05, ANOVA). **(C)** Quantification of basal epithelial cells in PTEN$^{L/L}$ and PTEN$^{L/L}$;4EBP1^M mice after doxycycline treatment (n = 6 mice/treatment arm, *P<0.0001, t-test). **(D)** Quantification of luminal epithelial cells in PTEN$^{L/L}$ and PTEN$^{L/L}$;4EBP1^M mice after doxycycline treatment (n = 6 mice/treatment arm, *P<0.0001, t-test). **(E)** Absolute quantification of 7AAD/Annexin-positive basal epithelial cells in in PTEN$^{L/L}$ and PTEN$^{L/L}$;4EBP1^M mice (n = 6-7/genotype, *P = 0.01, t-test). n.s. = not statistically significant. Data are mean +/- S.E.M.
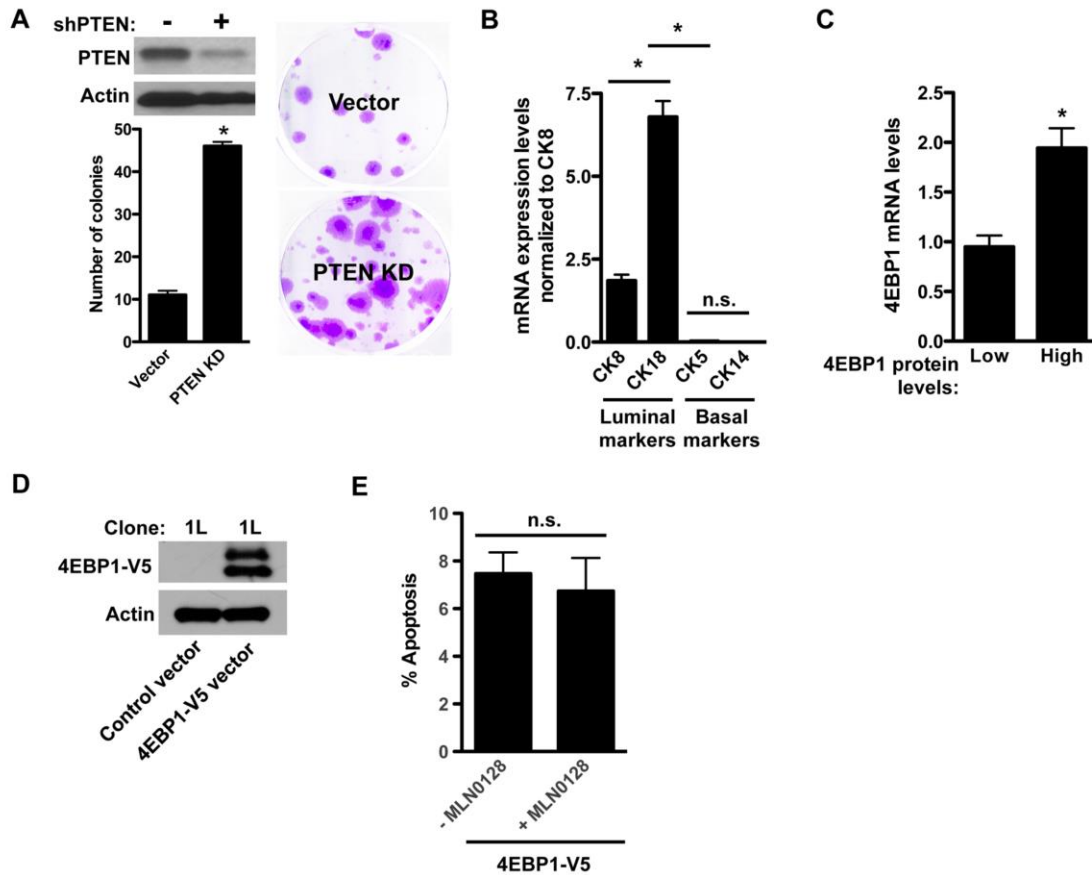
Figure S7. Expression of 4EBP1 endows resistance to MLN0128 in LHS PTEN KD cell lines. (A) Representative western blot analysis of SV40 large T, hTERT, and SV40 small T (LHS) immortalized primary prostate epithelial cells (PrEC) with and without stable PTEN knockdown (KD). Clonogenic assay of LHS PrEC cells with and without stable PTEN knockdown (KD) (assay done in duplicate, P = 0.0008, t-test). **(B)** qPCR-based phenotyping of PTEN KD LHS PrEC cells for CK8, CK18, C5, and CK14 epithelial markers (data based on 5 individual clones, *P<0.05, t-test). **(C)** Representative qPCR analysis of *4EBP1* mRNA expression in MLN0128-sensitive (low 4EBP1 protein abundance) and resistant (high 4EBP1 protein abundance) PTEN KD LHS PrEC clones (*P = 0.01, t-test). Both samples were normalized to actin. **(D)** Representative Western blot of low 4EBP1-expressing PTEN KD LHS PrEC 1L clone with and without overexpression of a wild-type 4EBP1 V5-tagged construct. **(E)**

Low 4EBP1-expressing PTEN KD LHS PrEC "clone 1L" cells were transfected with a wild-type V5-tagged 4EBP1 construct and treated with MLN0128 for 12 hours. Graph represents % propidium iodide- and annexin V-positive cells assessed by flow cytometry (a replicate of 6 experiments, assessed by a t-test). n.s. = not statistically significant. Data are mean +/- S.E.M.

A Pre-treatment Post-treatment

B

Patient	PSA, baseline (ng/dL)	PSA, post-BKM120 (ng/dL)
BKM-001	37.8	49.1
BKM-002	0.12	n/a
BKM-003	32	n/a
BKM-004	22	n/a
BKM-005	9	n/a
BKM-006	7.7	9.589
BKM-007	5.3	5.893
BKM-008	116	n/a
BKM-009	49	47.7
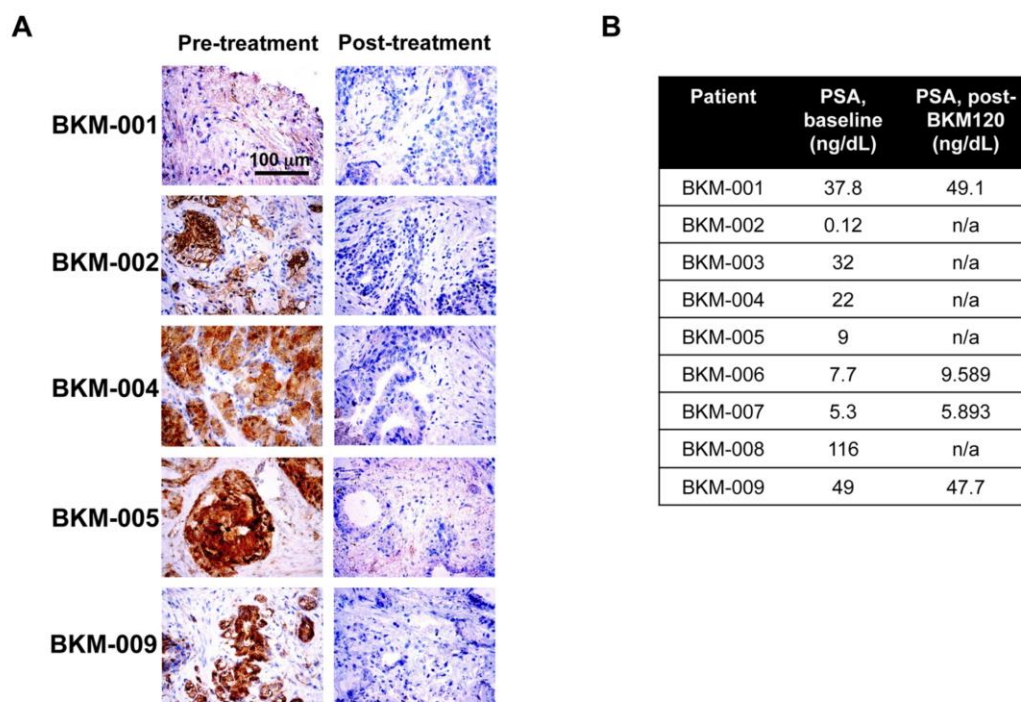
Figure S8. Phosphorylated AKT (Ser[473]) immunohistochemistry of prostate tumors and serum PSA concentrations from patients before and after treatment with BKM120. **(A)** Representative immunohistochemistry staining for phosphorylated AKT abundance in patients before and after treatment with BKM120. Scale bar, 100 μm. **(B)** Summary of patient characteristics in the phase 2 neoadjuvant BKM120 clinical trial. Of note, out of the 5 patients for whom pre- and post- treatment PSAs were collected, no objective PSA responses (>30% decrease in PSA) were observed (n/a = not available).

Target	Sequence (5'-3')
Mouse	
CK5	(f) ACCTTCGAAACACCAAGCAC
	(r) TTGGCACACTGCTTCTTGAC
CK14	(f) CCTCTGGCTCTCAGTCATCC
	(r) GAGCAGCATGTAGCAGCTT
p63	(f) GAGAGAGGGCATCAAAGGTG
	(r) GGAAAACAATGCCCAGACTC
CK8	(f) ATCGAGATCACCACCTACCG
	(r) CTGAAGCCAGGGCTAGTGAG
CK18	(f) AAGGTGAAGCTTGAGGCAGA
	(r) CTGCACAGTTTGCATGGAGT
Nkx3.1	(f) CTCCAGAGCCCGACAAAG
	(r) CACTTGCTAAGTCCCCTGGA
4EBP1	(f) AGAATGATCTGGCAATCCTAGC
	(r) TTCCTGTCAGGGAAAGAAGTAAA
4EBP1^{M}	(f) CAGGGTGTTGTTTAGAATGGGAA
	(r) GAGGAGACAATGGTTGTCAACAGA
PTEN	(f) AGGCACAAGAGGCCCTAGAT
	(r) CTGACTGGGAATTGTGACTCC
Actin	(f) CTAAGGCCAACCGTGAAAAG
	(r) ACCAGAGGCATACAGGGACA.
Human	
CK5	(f) GCAGATCAAGACCCTCAACAAT
	(r) CCACTTGGTGTCCAGAACCT
CK14	(f) CCTCCTCCCAGTTCTCCTCT
	(r) ATGACCTTGGTGCGGATTT
CK8	(f) AGGGCTGACCGACGAGAT
	(r) CACCACAGATGTGTCCGAGA
CK18	(f) TGATGACACCAATATCACACGA
	(r) GGGCTTGTAGGCCTTTTACTTC
4EBP1	(f) CAGGAAGTGGACAAGAACGAA
	(r) TCCCAAGCACATCAACCTAAG
Actin	(f) GCAAAGACCTGTACGCCAAC
	(r) AGTACTTGCGCTCAGGAGGA

Table S1: qPCR oligonucleotide sequences. The forward (f) and reverse (r) sequences for each qPCR oligonucleotide are provided.